International Journal of Nanomedicine

Dovepress
open access to scientific and medical research

Open Access Full Text Article

ORIGINAL RESEARCH

Toxicopathological and immunological studies on different concentrations of chitosan-coated silver nanoparticles in rats

This article was published in the following Dove Press journal:
International Journal of Nanomedicine

Eman Ibrahim Hassanen[1]
Abdelazeem Ali Khalaf[2]
Adel Fathy Tohamy[2]
Eman Ragab Mohammed[3]
Khaled Yehia Farroh[4]

[1]Department of Pathology, Faculty of Veterinary Medicine, Cairo University, Giza, Egypt; [2]Department of Toxicology & Forensic Medicine, Faculty of Veterinary Medicine, Cairo University, Giza, Egypt; [3]Department of Microbiology, Faculty of Veterinary Medicine, Cairo University, Giza, Egypt; [4]Nanotechnology & Advanced Materials Central Laboratory, Agricultural Research Center, Giza, Egypt

Background: Much consideration has been paid to the toxicological assessment of nanoparticles prior to clinical and biological applications. While in vitro studies have been expanding continually, in vivo investigations of nanoparticles have not developed a cohesive structure. This study aimed to assess the acute toxicity of different concentrations of chitosan-coated silver nanoparticles (Ch-AgNPs) in main organs, including liver, kidneys, and spleen.

Materials and methods: Twenty-eight male albino rats were used and divided into 4 groups (n=7). Group 1 was kept as a negative control group. Groups 2, 3, and 4 were treated intraperitoneally with Ch-AgNPs each day for 14 days at doses of 50, 25, and 10 mg/kg body weight (bwt) respectively. Histopathological, morphometric and immunohistochemical studies were performed as well as oxidative stress evaluations, and specific functional examinations for each organ were elucidated.

Results: It was revealed that Ch-AgNPs induced dose-dependent toxicity, and the repeated dosing of rats with 50 mg/kg Ch-AgNPs induced severe toxicities. Histopathological examination showed congestion, hemorrhage, cellular degeneration, apoptosis and necrosis in hepatic and renal tissue as well as lymphocytic depletion with increasing tangible macrophages in the spleen. The highest levels of malondialdehyde, alanine aminotransferase, aspartate aminotransferase (MDA, ALT, AST) and the lowest levels of reduced glutathione, immunoglobulin G, M and total protein (GSH, IgG, IgM, TP) were observed in this group. On the other hand, repeated dosing with 25 mg/kg induced mild to moderate disturbance in the previous parameters, while there was no significant difference in results of pathological examination and biochemical tests between the control group and those treated with 10 mg/kg bwt Ch-AgNPs.

Conclusion: Chitosan-coated silver nanoparticles induce dose-dependent adverse effects on rats.

Keywords: histopathology, oxidative stress, immunotoxicity, chitosan-coated silver nanoparticles, apoptosis

Introduction

Nanotechnology is the study of extremely small structures, having a size of 0.1–100 nm.[1] Nanoparticles (NPs) are used in a number of applications in the biomedical, bioengineering, and optical fields. Great attention has been given to the toxicology of NPs, which represent danger therapeutically and naturally. From a biomedical point of view, the toxicology of NPs uncovers the reaction between the physicochemical characteristics of NPs and their natural impacts. Appraisal of the damaging effects of NPs requires many

Correspondence: Adel Fathy Tohamy
Department of Toxicology and Forensic Medicine, Faculty of Veterinary Medicine, Cairo University, Gamaa Street, Giza, Cairo 12211, Egypt
Tel +20 100 557 1904
Fax +20 2 357 2540
Email adel_367@yahoo.com

submit your manuscript | www.dovepress.com
DovePress
http://doi.org/10.2147/IJN.S207644

configuration runs in either in vitro or in vivo examinations. Marquis et al[2] reviewed studies of proliferation, necrosis, apoptosis, DNA damage, and oxidative stress, which are related to the main mechanisms of cytotoxicity,[3] and stressed the significance of nanotoxicity in in vivo investigations.[3] Relatively long-term, complicated, and animal-sacrificed in vivo investigations come after vitro evaluations and are necessary before wide application.

Silver nanoparticles (AgNPs) are wildly used in medicine owing to their antimicrobial properties.[4] The toxicity of AgNPs remains to a great extent obscure and in vivo data of AgNP toxicities are particularly restricted and disputable.[5,6] AgNPs can be absorbed into the circulation by means of different routes of administration, prompting deposition of silver in many organs, mainly the liver and spleen, causing organ damage.[7–9] An ongoing report[10] recommended that short-term oral administration of high doses of AgNPs in rats (25–100 mg/kg) could significantly elevate reactive oxygen species (ROS), alanine aminotransferase (ALT), aspartate aminotransferase (AST), and lipid hydroperoxide, and cause DNA damage. On the other hand, a 28-day inhalation toxicity study (1.32×10^6 AgNPs/cm^3) noticed no changes in body weight or in the hematology and blood biochemical parameters of Sprague-Dawley (SD) rats.[11] Another report likewise proposed that SD rat oral gavage with up to 36 mg/kg AgNPs for 13 weeks showed no conspicuous changes in histopathology, hematology, clinical chemistry, micronuclei, and reproductive system parameters.[12] The toxicities that come from the different administration routes regularly fluctuated because of the distribution patterns. For instance, in a single-dose oral administration study,[13] the tissue distribution of Ag in the liver, kidneys, and lungs was higher when Ag^+ was administered compared with AgNPs. However, intravenously administered AgNPs predominantly aggregated in the liver and spleen, and the free Ag^+ was in this way released and excreted, a large amount of which remained in the kidneys, lungs, and brain.[14] It is therefore vital to demonstrate the distribution pattern of AgNPs vs Ag^+ and to investigate their toxic impacts.

A few investigations have shown that different surface stabilizers have important effects on AgNP cytotoxicity. Due to its great biocompatibility and antibacterial properties, chitosan is utilized as an active ingredient of topical wound materials.[15] Several studies reported that chitosan has been considered as a good stabilizer for AgNPs and promotes wound healing and the antimicrobial effects by AgNPs.[16] Moreover, chitosan-coated AgNPs (Ch-AgNPs) showed high effectiveness in killing common Gram-positive and Gram-negative bacteria, and fungi.[17,18] Compared with a higher degree of polymerization of chitosan, low molecular weight chitosan (LMWC) has better water solubility and biological activity,[19] recommending that LMWC may be an ideal stabilizer of AgNPs. Furthermore, a few researchers found that chitosan NPs incorporating silver have higher toxicity than those incorporating other metal ions such as magnesium, zinc, and copper.[20,21] Although numerous studies have summarized the methods in both in vitro and in vivo evaluations in certain nanostructures in various model frameworks, fundamental assessment stays inconclusive. Fischer[4] talked about the significance of creating prescient models of NP toxicity assessment, while other studies have concentrated on histological changes[22] and pharmacokinetic parameters like exposure,[23] bio-distribution, biochemistry metabolism, and clearance.[24]

Numerous investigations discussed the in vitro antimicrobial effects of Ch-AgNPs. However, investigation of its toxicity has been limited in laboratory animals. In this study, albino Wister male rats as a popular model were used to study the in vivo toxicities triggered by repeated Ch-AgNPs intraperitoneal administrations for 14 days. Furthermore, three different concentrations of Ch-AgNPs were likewise used to think about the toxicological contrasts between them. Our study will provide a comprehensive insight into the immunotoxicity induced in rats by Ch-AgNPs, which may contribute to a better understanding of the potential risk of Ch-AgNPs containing medical materials.

Materials and methods

Preparation of chitosan-coated silver nanoparticles

Chitosan (molecular weight 50,000–190,000 Da, degree of deacetylation 75–85% and viscosity 20–300 cP), glacial acetic acid, silver nitrate, sodium borohydride, and all the other chemicals were purchased from Sigma-Aldrich Co. (St Louis, MO, USA).

Ch-AgNPs were prepared by chitosan reduction of silver nitrate according to Babu et al (2017).[25] Silver ions are being coordinated by amino groups of polymeric chains in chitosan acidic solution. Ions reduction to metallic silver NPs is coupled with chitosan hydroxyl group oxidation. Briefly, chitosan aqueous solution (1% w/v) was prepared by dissolving chitosan in acetic acid solution (1% v/v) at room temperature. Subsequently, the silver nitrate solution (0.01 M) was added immediately into the

suspension under stirring for 2 h. Sodium borohydride (20 mL, 0.04 M) was added to the previous suspension and an immediate color changes from pale yellow to brown. The resulting Ch-AgNP suspension was centrifuged at 20,000 g for 30 min. The pellet was resuspended in deionized water. The Ch-AgNP suspension was freeze-dried before further use or analysis.

Characterization of the prepared nanoparticles

The crystalline and phase structure of the synthesized NPs was studied by an X-ray diffractometer (XRD, X'Pert Pro, Malvern Panalytical Ltd, Malvern, UK). The size (Z-average mean) and zeta potential of the NPs were analyzed by photon correlation spectroscopy and laser doppler anemometry, respectively, in triplicate using a Zetasizer 3,000HS (Malvern Instruments, Malvern, UK). The morphology and size were determined by the transmission electron microscopy (TEM, Tecnai G20, FEI, Netherlands). All the preparation and characterization processes were conducted at Nanotechnology and Advanced Materials Central Lab (NAMCL), Agricultural Research Center, Egypt.

Animals and experimental design

All procedures were conducted in accordance with the guidelines contained in the guide for the care and use of laboratory animals 8th edition 2011 (the guide). The protocol was approved by the Institutional Animal Care and Use Committee at Cairo University (IACUC, CU-II-F-10-19), Cairo, Egypt. Twenty-eight male albino Wister rats weighing 170–200 g were obtained from the Department of Veterinary Hygiene and Management's animal house, Faculty of Veterinary Medicine, Cairo University. All animals were housed in plastic cages (4 or 3 rats/cage) in a well-ventilated environment and received a daily illumination of 16 h of light. They were fed on dry commercial standard pellets with access to tap water ad libitum throughout the experimental period. They were acclimatized to the environment for 2 weeks prior to the onset of the experiment to ensure their healthy state.

Rats were randomly divided into four groups (n=7). Group 1 was kept without any treatment except i.p. injection of normal saline. Groups 2, 3, and 4 were administered different concentrations of Ch-AgNPs intraperitoneally, each day for 14 days at doses of 50, 25, and 10 mg/kg body weight (bwt), respectively. Doses of NPs were selected according to previous studies.[26]

Sampling

At the end of the experiment, blood samples were collected from all rats in the different groups. Centrifugation was performed at 4,500 RPM for 5 min to obtain clear serum samples then preserved at −20°C till use for biochemical and immunological tests.

Rats were euthanized at the end of the experiment by cervical dislocation, and the main organs including liver, kidneys, and spleen were collected. Some of these organs were preserved in 10% neutral buffered formalin for histopathological and immunohistochemical studies, while others were preserved at −20°C for oxidative stress evaluations.

Clinical chemistry

ALT, AST, blood urea nitrogen, creatinine, and total protein were analyzed according to the instructions of the commercial kits (Biodiagnostic Co., Giza, Egypt).

Hematology

Blood was collected in EDTA-coated tubes. All hematology parameters were determined utilizing an Erma Hematology Analyzer (Tokyo, Japan). These parameters were white blood cell (WBC) count, red blood cell (RBC) count, hemoglobin (HGB) and platelet (PLT) count. In addition, the number and percentage of monocytes and lymphocytes were measured. Then, blood smears were prepared for visual evaluation.

Immunoglobulin levels

After collection of blood serum, immunoglobulin levels were determined using ELISA using mouse monoclonal antibodies against rat IgG and IgM, respectively, as described in the manufacturer kit (Biocheck Inc., Foster City, CA, USA). Briefly, serum samples were incubated with mouse monoclonal antibodies against rat IgG and IgM, 1:5,000 and 1:3,000, respectively, for 30 min at 37°C. The plates were washed and tetramethylbenzidine substrate was added and incubated for 10 min in the dark at room temperature (RT). The reaction was stopped with 10% (w/v) H_2SO_4. Optical density was measured at 490 nm using a Spectramax 190 spectrophotometer (Molecular Devices, Sunnyvale, CA, USA).

Histopathology and morphometric studies

Tissue specimens from liver, kidneys, and spleen were collected then fixed in 10% neutral buffered formalin (pH 7.0) and processed by the conventional methods to obtain paraffin sections. The embedded paraffin sections

were cut at 4.5 μm then stained by H&E stain for histopathological examination.[27]

Microscopic grading and scoring of the spleen, liver, and kidney tissue sections were carried out to determine the degree of severity of the observed histopathological lesions according to Baliga et al[28] but with some modifications. Grading of both hepatocellular and renal damage was performed according to the following parameters: epithelial cell degeneration, necrosis, vascular congestion, hemorrhage, and inflammatory cell infiltration. Grading of the splenic injury was performed according to the following parameters: lymphoid cell atrophy, reticular cells hyperplasia, tangible body macrophages, and splenic hemorrhage. The above parameters were assessed and scored as mild, moderate, and severe, as follows: (−) normal histology; (+) mild <25%; (++) moderate 25–50%; (+++) severe >50% of the tissues affected.

Immunohistochemistry

Immunohistochemical studies were performed to detect caspase-3 and PCNA protein expressions on paraffin spleen, liver, and kidney tissue sections using an immunoperoxidase test as mentioned by Hsu et al.[29] Briefly, tissue sections were incubated with a primary antibody (Dako Corp., Carpinteria, CA, USA) and reagents required for the avidin-biotin peroxidase (Vactastain ABC peroxidase kit, Vector Laboratories, Burlingame, CA, USA) test for the detection of the antigen–antibody complex. Each immunohistochemical marker was treated by the chromogen 3, 3-diaminobenzidine tetrahydrochloride (DAB, Sigma Chemicals, Perth, Australia) and counterstained by hematoxyline then examined under a light microscope.

Immunohistochemical reactions were quantified using Image J software. Morphometric results expressed as a percentage of specific positive area in relation to the total counted area and measured as mean ± SEM.

Oxidative stress markers

Liver, kidney, and spleen samples were evaluated for lipid peroxidation, expressed by malondialdehyde (MDA) formation, as described by Ohkawa et al[30] and reduced glutathione (GSH) levels were assessed as described by Beutler et al[31] using commercial kits (Biodiagnostics, Cairo, Egypt).

Statistical analysis

Statistical analysis was performed with SPSS version 16.0 software (SPSS Inc., Chicago, IL, USA). Data were expressed as means ± standard error of mean (SEM). Comparison of means was performed by one-way ANOVA followed by independent-sample Student's *t*-test. A value of $P \leq 0.05$ was considered statistically significant.

Results

Characterization of chitosan-silver nanoparticles

X-ray diffraction (XRD) pattern of Ch-AgNPs

The XRD pattern of the prepared Ch-AgNPs was graphically illustrated in Figure 1A. The presence of chitosan, silver and the absence of impurity phases was evident from the XRD image. The peak for chitosan appeared at a 2θ value of the broad peak around 15–35°. The peaks of silver were indexed to the face-centered cubic structure which is in good agreement with the JCPDS card No. 04-004-8730. The three silver peaks obtained belong to the (111), (220) and (311) reflections, respectively. The results showed that the synthesized NPs were AgNPs because the position and relative intensity of all the diffraction peaks of the samples were consistent with the crystalline pattern of silver.

Dynamic light scattering (DLS) analysis

DLS was used to measure the hydrodynamic diameter in the nanometer range. The size of Ch-AgNPs was 20 nm, and zeta potential was 66 mV as shown in Figure 1B and C.

High-resolution transmission electron microscope (HR-TEM) analysis

HR-TEM gave us information on the particle shape and the determination of particle size. The results of TEM, shown in Figure 1D, indicate that the Ch-AgNPs were spherical with particle size in the range of 17±5 nm, distributed homogeneously in the Ch matrix.

Clinical chemistry and hematology

There was a significant increase of serum levels of ALT, AST, blood urea nitrogen, and creatinine, and a significant decrease in levels of total protein in the group treated with 50 mg/kg bwt of Ch-AgNPs compared to other groups, as illustrated in Figure 2. Levels of the above biochemical parameters were similar without any significant difference in other groups.

In general, minor alterations were observed in hematological parameters (Table 1). For blood, several parameters

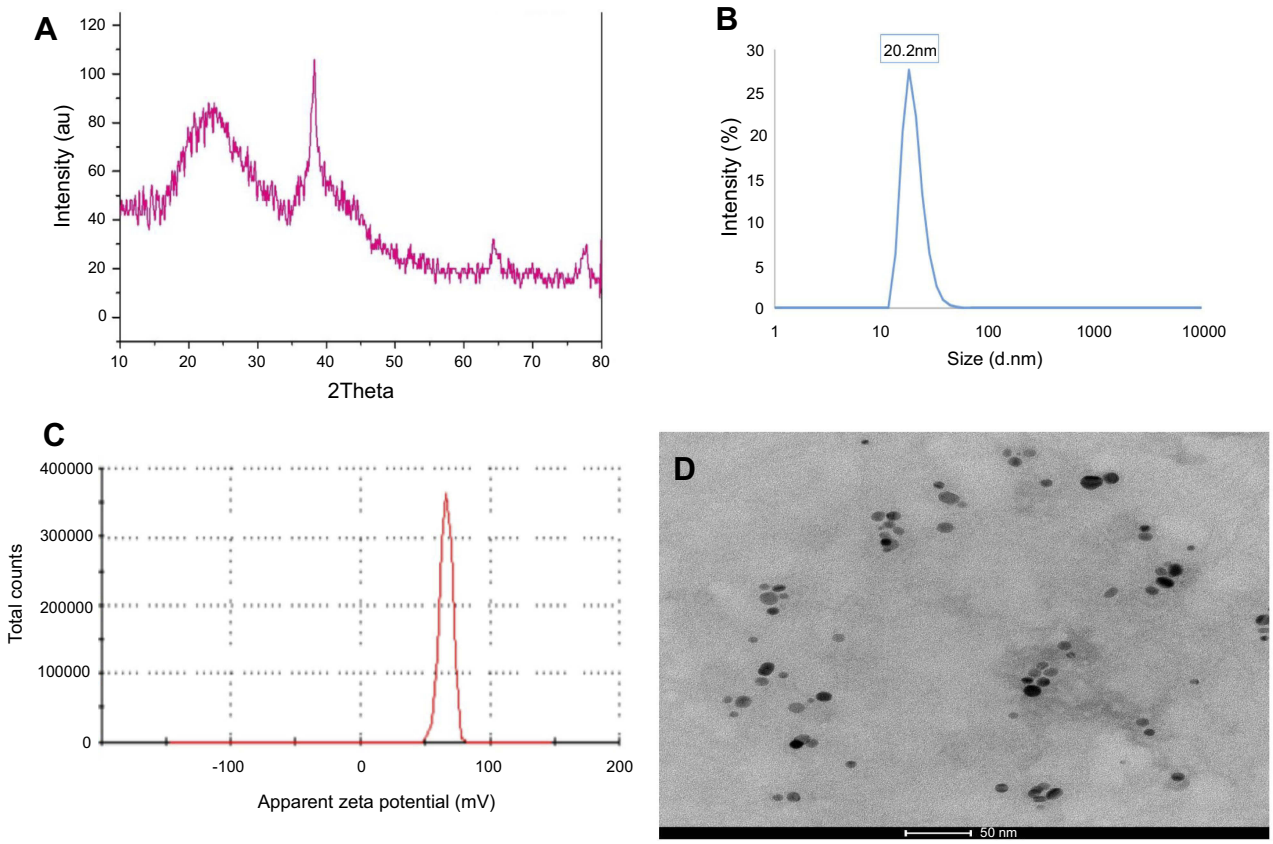

Figure 1 (**A**) X-ray powder diffraction patterns of Ch-AgNPs. (**B** and **C**) Dynamic light scattering analysis of Ch-AgNPs. Particle size was 20 nm (B), and zeta potential 66 mV (C). (**D**) High-resolution transmission electron microscope image of Ch-AgNPs showing spherical NPs with particle size in the range of 17.5 nm distributed homogeneously in the Ch matrix.
Abbreviation: Ch-AgNPs, chitosan-coated silver nanoparticles.

associated with red blood cell generation showed a significant decrease in the highest dose administered which could be confirmed by reduced hemoglobin (Hb) level in the group that received 50 mg/kg Ch-AgNPs. The total number of WBC, PLT count and lymphocytes were significantly decreased in the highest dose.

Immunoglobulin level

There was a significant decrease in the levels of IgG in groups that received the highest and the moderate dose compared with those that received the lowest dose and the control group. Levels of IgM were quite similar to each other without any significant difference, as shown in Figure 2.

Histopathological pictures

Microscopic examination of the spleen tissue sections in the control group showed normal histological structures (Figure 3A), while rats administered Ch-AgNPs showed dose-dependent pathological alterations. Lesions are restricted to groups of rats receiving 50 mg/kg Ch-AgNPs. There were congestion and fibrinoid necrosis of follicular arteries associated with follicular hemorrhage (Figure 3B). The most prominent observable lesions were severe atrophy and necrosis of the lymphoid cells with hyperplasia of reticular cells (Figure 3C). Numerous apoptotic cells surrounded by clear space and multiple tangible body macrophages were also recorded. A large amount of eosinophilic hyaline material and fibrin threads fill the sinusoids and replace the splenic parenchyma (Figure 3D). Hemosederin pigment was detected in red and white pulp in some cases (Figure 3E). Perisplenitis was observed in some cases and was characterized by congestion, fibrin deposition and mononuclear inflammatory cell infiltrations in the splenic capsule (Figure 3F). Rats treated with 25 mg/kg Ch-AgNPs showed mild to moderate depletion of lymphocytes within lymphoid follicles (Figure 3G). The spleen of rats treated with 10 mg/kg Ch-AgNPs showed normal histology. Lymphoid follicles appeared with normal histology (Figure 3H) without any depletion of the lymphocytes.

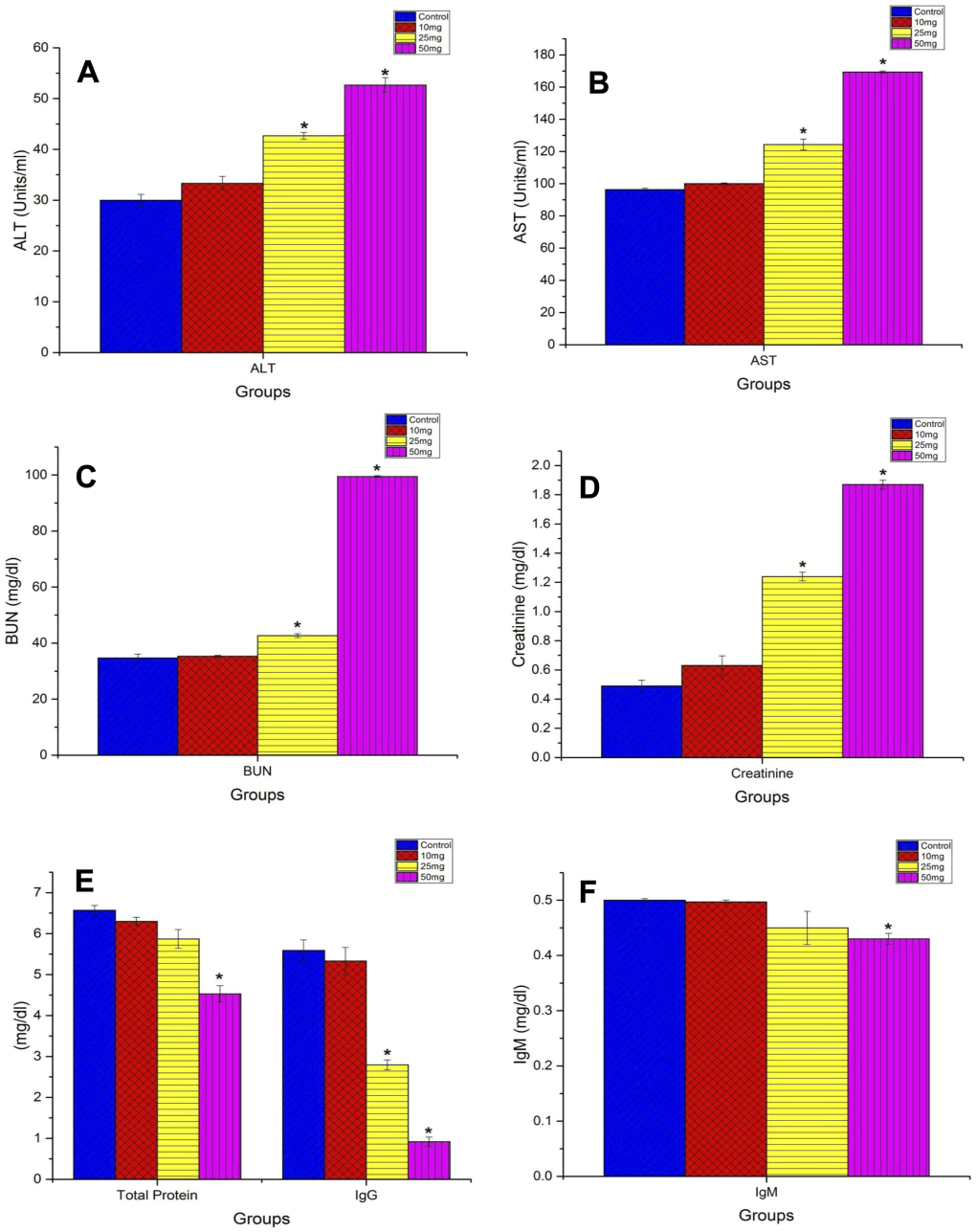

Figure 2 Serum levels of (**A**) ALT, (**B**) AST, (**C**) BUN, (**D**) creatinine, (**E**) total protein and IgG, and (**F**) IgM in different groups. Data are represented as mean ± SEM. *Indicates significant difference from the corresponding control group at $P \leq 0.05$.

Abbreviations: ALT, alanine aminotransferase; AST, aspartate aminotransferase; BUN, blood urea nitrogen.

In contrast to normal control rats (Figure 4A), those treated with 50 mg/kg Ch-AgNPs showed moderate hepatocellular injury with remarkable diffuse vacuolar degeneration (Figure 4B). The hepatocytes appeared swollen with pale vacuolar cytoplasm. Individual hepatocellular necrosis and apoptosis were also detected (Figure 4C). Multifocal areas of hemorrhage were recorded in the hepatic parenchyma (Figure 4D). There was fibrinous perihepatitis characterized by congestion of the blood vessels, and mononuclear inflammatory cell infiltration with faint pink fibrin threads in the Glissonian capsule (Figure 4E). Multifocal areas of hepatocellular coagulative necrosis infiltrated with mononuclear inflammatory cells were detected. The cytoplasm of hepatocytes appeared deeply eosinophilic with pyknotic nuclei. Only hyperactivation of the Kuppfer cells and binucleated hepatocytes were noticed in groups treated

Table 1 Hematological parameters of rats in different groups

Parameters	G1	G2	G3	G4
RBCs (millions/cmm)	7.9±0.05	7.08±0.04 *	7.4±0.05 *	7.68±0.04
Hb (g/dl)	15.33±0.09	13.47±0.23*	14.03±0.03*	14.77±0.23
PLAT (thousands/cmm)	960±10	244.67±0.03*	365.33±2.91*	886±33.53
TWBCs (thousands/cmm)	11.63±0.22	5.8±0.1*	9.23±0.07*	11.37±0.4
LQ %	71.1±0.06	51.13±0.13*	61.9±0.56*	70.93±0.99
MQ %	17.53±0.15	18.73±0.09*	18.67±0.03*	17.77±0.37

Note: *Indicates significant difference from the corresponding control group at $P \leq 0.05$.
Abbreviations: G1, control group; G2, group receiving 50 mg/kg Ch-AgNPs; G3, group receiving 25 mg/kg Ch-AgNPs; G4, group receiving 10 mg/kg Ch-AgNPs; RBCs, red blood cells; Hb, hemoglobin; PLAT, platelet count; TWBCs, total white blood cells; LQ, lymphocytes; MQ, macrophage.

with 25 and 10 mg/kg Ch-AgNPs without any pathological alterations (Figure 4F and G).

In contrast to the control (Figure 5A), kidneys of rats treated with 50 mg/kg Ch-AgNPs had severe to moderate histopathological alterations. The main lesion observed was acute focal interstitial nephritis (Figure 5B). There were congestion of interstitial blood vessels and glomerular capillary tuft. Degeneration of renal tubular epithelial cells was observed and associated with hemorrhage in between renal tubules (Figure 5C). Focal interstitial inflammatory cell infiltration was detected. Some renal tubules contained cellular hyaline cast in their lumen. Necrosis of renal tubular epithelial cells was mostly observed with the complete destruction of the renal tubules (Figure 5D). Kidneys of rats administered 25 mg/kg Ch-AgNPs showed severe congestion with mild degeneration and necrosis in the renal tubular epithelium (Figure 5E); while those administered 10 mg/kg Ch-AgNPs had normal histology (Figure 5F).

Results of the microscopic scoring shown in Tables 2–4 revealed severe to moderate histopathological alterations in all of the examined organs (spleen, liver, kidneys) in the group treated with 50 mg/kg Ch-AgNPs. Moderate pathological alterations were observed in the group treated with 25 mg/kg Ch-AgNPs. On the other hand, the mildest lesions were observed in groups treated with 10 mg/kg Ch-AgNPs.

Immunohistochemical examinations

Results of immunohistochemical staining of the spleen, liver, and kidney tissue sections are summarized in Table 5 and illustrated in Figures 6–8. There was marked positive expression of caspase-3 (an immunohistochemical marker for apoptosis) among the lymphoid cells in the splenic follicles, hepatocytes, the epithelial lining of bile ducts and in the renal tubular epithelial cells in groups treated with 50 mg/kg Ch-AgNPs. Mild positive to negative expression of the apoptotic marker (caspase-3) was noticed in spleen, liver, and kidney sections in rats treated with either 25 or 10 mg/kg Ch-AgNPs.

The protein expression of PCNA (as an immunohistochemical marker for proliferation) (Figures 6 and 8) was significantly elevated in the spleen of rats administered either 25 or 10 mg/kg Ch-AgNPs compared to the corresponding control group. At the same time, the expression of this proliferating protein marker did not differ between other groups.

All of the above immunohistochemical markers showed normal mild positive to negative expression in rats of the control group.

Oxidative stress markers

Rats exposed to Ch-AgNPs showed a dose-dependent increase in MDA level and a decrease in GSH content in different organs (liver, kidneys, and spleen). The rats exposed to 50 mg/kg bwt. showed a significant decrease in the level of the GSH content in comparison to the corresponding control group ($P \leq 0.05$) (Figure 9A); in addition, the MDA level showed a significant increase in liver, kidney, and spleen in comparison to the control group ($P \leq 0.048$) (Figure 9B). There was no significant difference in the levels of MDA and GSH between the control group and those treated with either 25 or 10 mg/kg Ch-AgNPs.

Discussion

AgNPs are amongst the most broadly connected nano material in the biomedical and pharmacological fields, and this leads to worries about security controls and the danger related to discharging organically dynamic Ag+ into the human body.[32] Appraisals of AgNP toxicity are limited, and restricted to the cytotoxicity and genotoxicity of silver particles in tissue cultures and cell lines.[33] Numerous in vitro investigations propose that the AgNPs

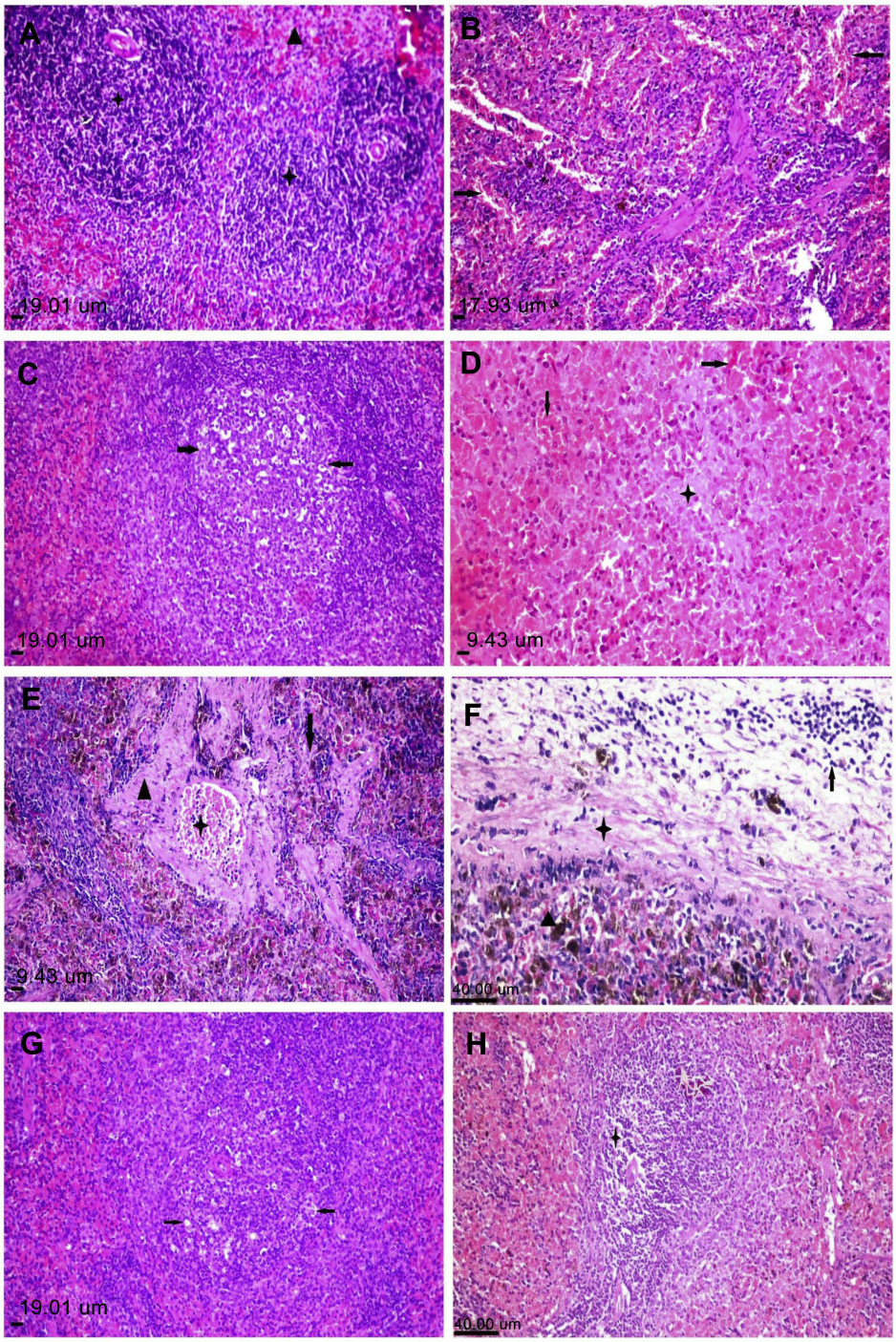

Figure 3 Histopathological alterations in splenic sections of rats in different groups. (**A**) Spleen of rat in the control group showing normal histology of both red (arrowhead) and white pulp (star). (**B**–**F**) Spleen of rat in the group that received 50 mg/kg Ch-AgNPs, showing (**B**) splenic hemorrhage (arrows) with hemosiderin pigment deposition in the red pulp; (**C**) lymphoid cell depletion with presence of many tangible body macrophages (arrows) detected within the splenic periarteriolar lymphoid follicles; (**D**) splenic hemorrhage (arrows) and fibrin threads (star) fill the splenic sinusoids in the red pulp; (**E**) deposition of hemosiderin pigment in the splenic parenchyma as well as congestion of central artery (star) with extensive lymphoid depletion (arrow) associated with reticular cell hyperplasia (arrowhead) in the white pulp; (**F**) thickening of the splenic capsule by fibrin deposition (star), edema and mononuclear inflammatory cell infiltrations (arrow). **(G)** Spleen of rat in the group that received 25 mg/kg Ch-AgNPs showing mild lymphoid depletion in the splenic lymphoid follicles. (**H**) Spleen of rat in the group that received 10 mg/kg Ch-AgNPs showing normal histology of both white (star) and red pulp.
Note: All sections stained by H&E.

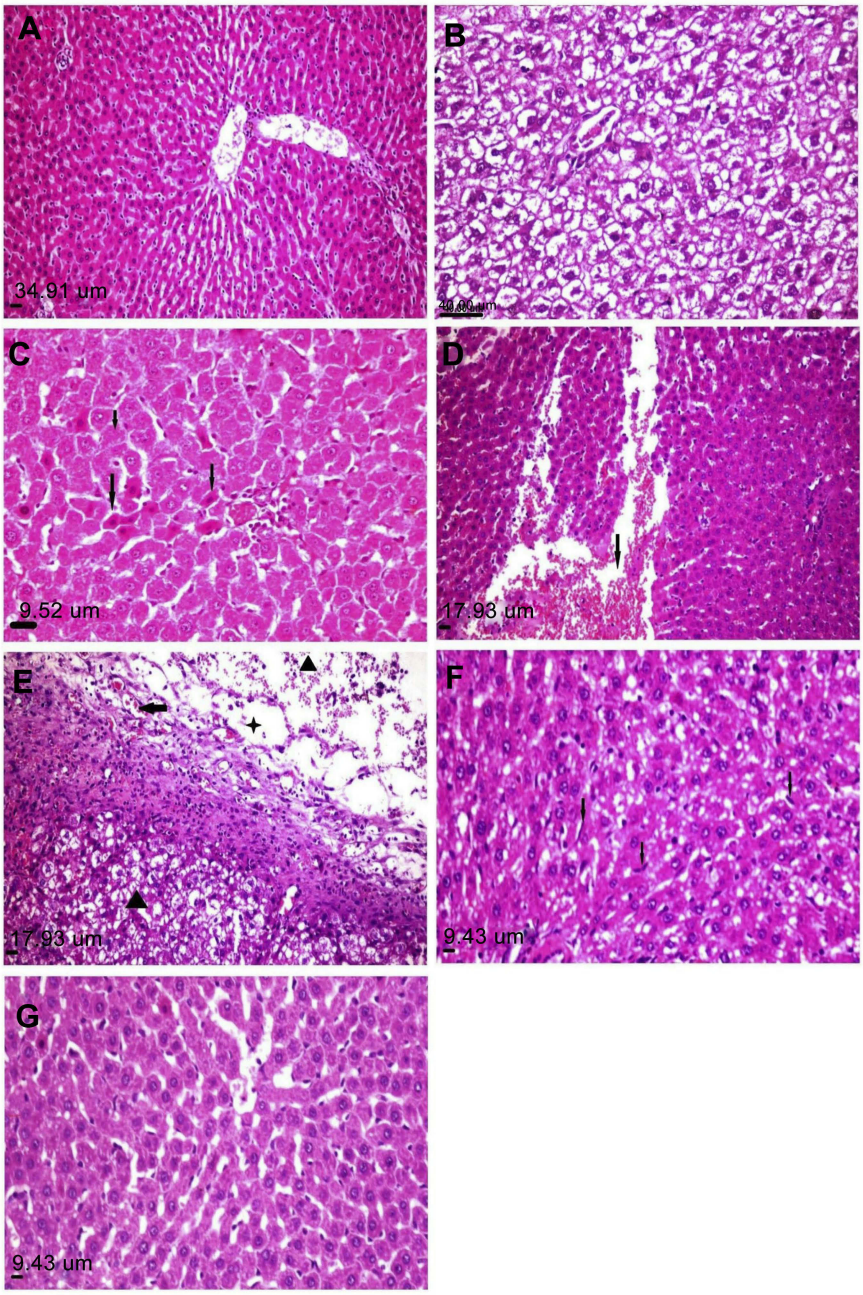

Figure 4 Histopathological alterations in liver tissue sections of rats in different groups. (**A**) Liver section of rat in the control group showing normal histology with normal central vein and hepatocytes arranged in the hepatic cords. (**B**–**E**) Liver sections of rats in the group that received 50 mg/kg Ch-AgNPs, showing: (**B**) diffuse hepatocellular vacuolar degeneration; (**C**) individual hepatocellular necrosis and apoptosis (arrow); (**D**) focal area of hemorrhage (arrow) in the hepatic parenchyma; (**E**) perihepatitis characterized by congestion (arrow), fibrin deposition (star) and inflammatory cells infiltration in the hepatic capsule together with hepatocellular vacuolar degenerations (arrowhead). (**F**) Liver of rat in the group that received 25 mg/kg Ch-AgNPs showing mild hepatocellular vacuolation with hyperactivation of Kupffer cells (arrow). (**G**) Liver of rat in the group that received 10 mg/kg Ch-AgNPs showing normal histology.
Note: All sections stained by H&E.
Abbreviation: Ch-AgNPs, chitosan-coated silver nanoparticles.

prompted dose- and size-dependant cytotoxic impacts on tissue cells. Kim et al[34] revealed that small-sized AgNPs (10 nm size) had a more prominent capacity to incite apoptosis in MC3T3-E1 cells than large-sized AgNPs (50 and 100 nm). Previous studies have shown that small-sized AgNPs are more toxic than large ones.[35,36] In an ongoing report, Ivask et al[37] confirmed the size-dependent toxic effects of AgNPs on several microbial species, protozoans, algae, crustaceans, and mammalian cells in vitro. The cytotoxicity of AgNPs could be influenced by particle

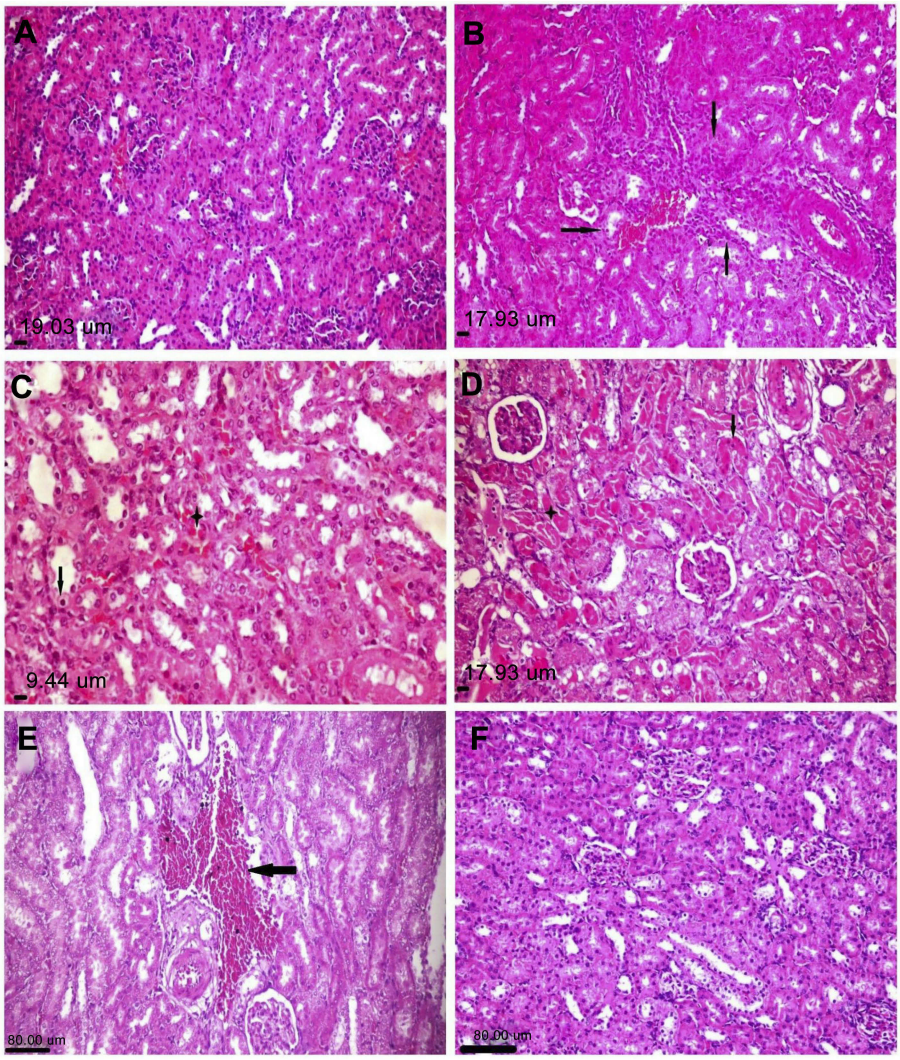

Figure 5 Histopathological alterations in the kidney tissue sections of rats in different groups. (**A**) Kidneys of rat in the control group showing normal glomerular and tubular histology. (**B–D**) Kidneys of rats in the group that received 50 mg/kg Ch-AgNPs, showing: (**B**) congestion, focal interstitial inflammatory cells infiltration together with degeneration and necrosis of renal tubular epithelium (arrow); (**C**) vacuolar degeneration in tubular epithelial cells (arrow) together with peritubular hemorrhages; (**D**) extensive necrosis in tubular epithelium together with hyaline cast (star) and necrotic cell debris (arrows) in tubular lumen. (**E**) Kidney sections of rat in the group that received 25 mg/kg Ch-AgNPs, showing severe congestion (arrow) with mild degeneration of the renal tubular epithelium. (**F**) Kidneys of rat in the group that received 10 mg/kg Ch-AgNPs showing normal histology.
Note: All sections stained by H&E.
Abbreviation: Ch-AgNPs, chitosan-coated silver nanoparticles.

Table 2 Microscopic grading and scoring of the spleen injury in rats of different groups

Groups/parameters	G1	G2	G3	G4
LQ atrophy	–	+++	+	–
RC hyperplasia	–	+++	+	–
Tangible MQ	+	+++	++	+
Hemorrhage	–	++	–	–

Notes: (–), normal; (+), mild; (++), moderate; (+++), severe
Abbreviations: G1, control group; G2, group receiving 50 mg/kg Ch-AgNPs; G3, group receiving 25 mg/kg Ch-AgNPs; G4, group receiving 10 mg/kg Ch-AgNPs; LQ, lymphocytes; RC, reticular cells; MQ, macrophages.

Table 3 Microscopic grading and scoring of the hepatocellular damage in rats of different groups

Groups/parameters	G1	G2	G3	G4
HCD	–	++	+	–
HCN	–	++	+	–
Hemorrhage	–	+	–	–
ICI	–	+	–	–

Notes: (–), normal; (+), mild; (++), moderate.
Abbreviations: G1, control group; G2, group receiving 50 mg/kg Ch-AgNPs; G3, group receiving 25 mg/kg Ch-AgNPs; G4, group receiving 10 mg/kg Ch-AgNPs; HCD, hepatocellular degenerations; HCN, hepatocellular necrosis; ICI, inflammatory cell infiltration.

Table 4 Microscopic grading and scoring of the renal damage in rats of different groups

Groups/parameters	G1	G2	G3	G4
TCD	+	+++	+	+
TCN	–	++	–	–
Renal cast	–	++	–	–
Congestion	–	++	+	–
Hemorrhage	–	++	–	–
ICI	–	+	–	–

Notes: (–), normal; (+), mild; (++), moderate; (+++), severe.
Abbreviations: G1, control group; G2, group receiving 50 mg/kg Ch-AgNPs; G3, group receiving 25 mg/kg Ch-AgNPs; G4, group receiving 10 mg/kg Ch-AgNPs; TCD, tubular cell degeneration; TCN, tubular cell necrosis; ICI, inflammatory cell infiltration.

Table 5 Quantitative analysis of positive caspase-3 protein expressions in the spleen, liver, and kidney sections in different groups

	G1	G2	G3	G4
Spleen	0.5±0.2	60±5.6*	25±5*	0.9±0.6
Liver	1.9±1.1	65±10*	45±3.1*	5±2.5
Kidneys	0.6±1.1	25±2.5*	5±3.1	5±2.2

Note: *Indicates significant difference from the corresponding control group at $P \leq 0.05$.
Abbreviations: G1, control group; G2, group receiving 50 mg/kg Ch-AgNPs; G3, group receiving 25 mg/kg Ch-AgNPs; G4, group receiving 10 mg/kg Ch-AgNPs.

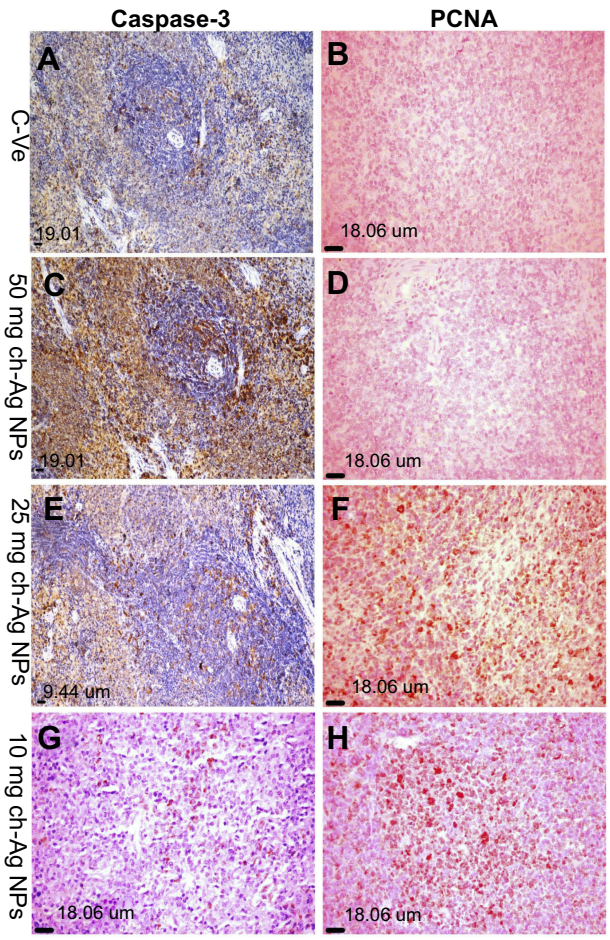

Figure 6 Immunohistochemical expression of caspase-3 and PCNA in the spleen sections in different groups showing negative caspase-3 and PCNA protein expression in the control negative group (**A** and **B**). Strong positive caspase-3 and negative PCNA protein expression in the group treated with 50 mg/kg bwt Ch-AgNPs (**C** and **D**). Moderate positive caspase-3 and PCNA protein expression in the group treated with 25 mg/kg bwt Ch-AgNPs (**E** and **F**). Negative caspase-3 and mild positive PCNA protein expression in the group treated with 10 mg/kg bwt Ch-AgNPs (**G** and **H**).
Abbreviations: bwt, body weight; Ch-AgNPs, chitosan-coated silver nanoparticles.

size, surface-stabilizing agents, pH, and some other factors.[5,8,38,39] Size, dose, and composition are properties of great importance in evaluation of nanotoxicity, and the surface-stabilizing coating is one of the most critical variables for shielding cell viability from AgNPs.[40,41] A few investigations have demonstrated that chitosan has good biocompatibility and antibacterial properties. However, few investigations examine the toxicity of Ch-AgNPs.

Oxidative stress is a key mechanism inducing cytotoxicity through enhancing the production of MDA accompanied by depletion of GSH in tissues; these are considered the most important indexes of antioxidant activities.[42] This may be a mechanism for the toxicity of NPs.[43,44] Many physiological and cellular events are induced by oxidative stress, including inflammation, DNA damage, and apoptosis.[45]

In the present study, after 14 days exposure to various concentrations of Ch-AgNPs in rats, doses of 50 mg/kg bwt caused a significant increase in MDA level and a significant decrease in GSH content in different organs (liver, kidney, and spleen). These results suggest that Ch-AgNPs may induce oxidative damage through a ROS-mediated process. AgNP toxicity seems to increase ROS production, as reported by Christensen et al.[41] The data are in accordance with Schlinkert et al[46] who stated that silver and gold NPs induced a significant increase in ROS production with an increase in chitosan coating. It was concluded that mechanisms of AgNP toxicity induce oxidative stress.[47] In the present study, Ch-AgNPs induced a significant elevation in LPO and depletion of GSH, which is in accordance with previous investigations.[36,48,49] GSH is considered as the first line of the cellular defense mechanism against oxidative damage. In this study depletion of GSH and an increased level of LPO may be how AgNPs induced cytotoxicity in different tissues (liver, kidney, and spleen) of exposed rats.

In contrast, Hajji et al[50] reported that low molecular weight Ch-AgNPs have antioxidant properties and are

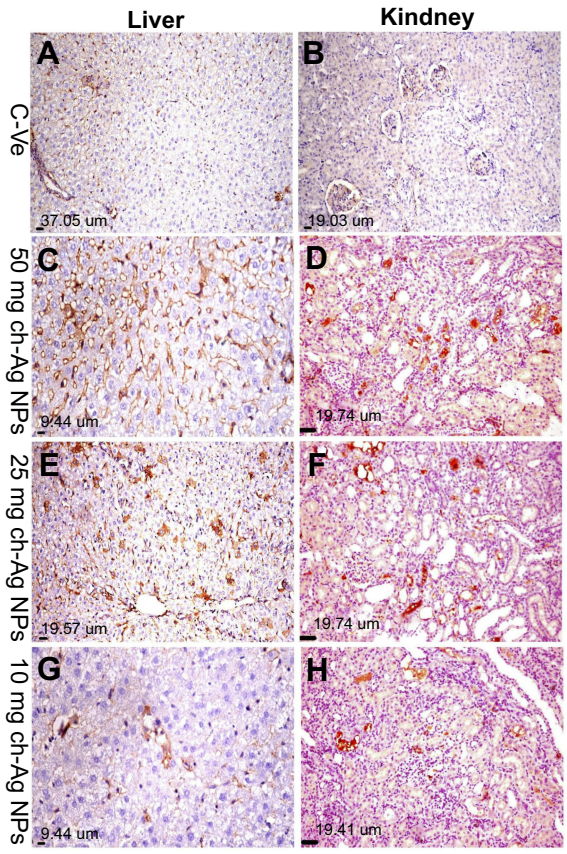

Figure 7 Immunohistochemical expression of caspase-3 in liver and kidney sections in different groups showing negative caspase-3 expressions in control negative group (**A** and **B**). Strong positive caspase-3 reactions in the group treated with 50 mg/kg bwt Ch-AgNPs (**C** and **D**). Moderate positive caspase-3 reaction in the group treated with 25 mg/kg bwt Ch-AgNPs (**E** and **F**). Mild positive to negative caspase-3 expression in the group treated with 10 mg/kg bwt Ch-AgNPs (**G** and **H**).
Abbreviations: bwt, body weight; Ch-AgNPs, chitosan-coated silver nanoparticles.

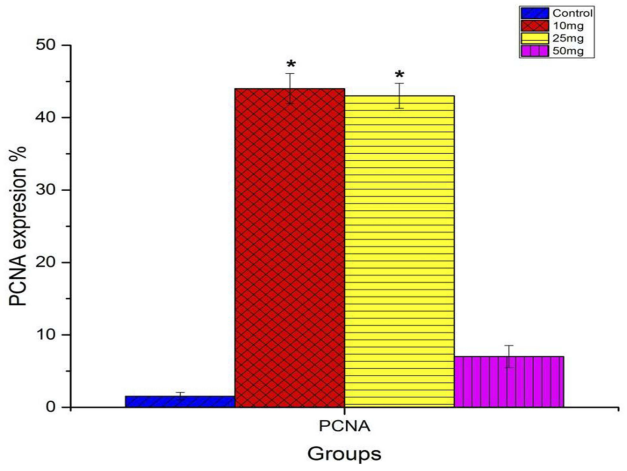

Figure 8 Image analysis of positive PCNA reactions in the spleen tissue sections in different groups. Data are represented as mean ± SEM. *Indicates significant difference from the corresponding control group at $P \leq 0.05$.

characterized by low cytotoxicity and promote wound healing. This difference may be related to the difference in concentrations, route of administration and method of preparation of the NPs.

Our outcomes demonstrated a significant increase in serum levels of urea nitrogen and creatinine in the group that received 50 mg/kg Ch-AgNPs, suggesting that renal damage caused disturbance in the elimination of both breakdown products through the kidneys, as recorded by Fatima et al51 There was a likewise critical rise in hepatic enzymes (ALT and AST) in this group, which demonstrates liver injury; it has recentlybeenfound that AgNP administration causes deterioration in hepatic functions.[52] The changes observed in the kidneys and liver biochemical parameters were confirmed by histopathological alterations and immunohistochemical examinations. In the present study, kidneys of rats treated with 50 mg/kg Ch-AgNPs showed focal interstitial nephritis, tubular epithelial degeneration, and necrosis with renal casts and showed strong positive expression of caspase-3 in the renal tubular epithelium. The most prominent pathological lesions observed in the liver were hepatocellular vacuolar degeneration and necrosis as well as strong positive caspase-3 protein expression noticed among hepatocytes. AgNPs could enter the host body by several routes and introduce injuries in the liver, kidneys,[53] spleen, lungs,[54] and the central nervous system.[55] Parang and Moghadamina[56] reported more cellular damage in the liver of rats exposed to AgNPs at a dose level of 100 mg/kg, in the form of swelling of cytoplasm, nuclear swelling, vacuole formation, abnormal hemorrhage, cellular congestion, and necrosis. These lesions were accompanied with elevation in serum ALT and AST.

Liver and kidneys are considered the targets of AgNPs in rats via oral or intraperitoneal administration.[57,58] The potential systemic toxicity of AgNPs remains dubious. Our results correlated with the data obtained by Al Gurabi et al[59] revealing that AgNPs induce a significant increase in symptoms of hepatic damage such as elevation in the level of ALP, ALT and AST enzymes. Guo et al[60] also noted that i.v. injection of AgNPs leads to the intoxication of liver and kidney organs through reducing the endothelial interconnection related to intracellular ROS. A few investigations affirmed that oral administration of Ch-AgNPs demonstrated no detectable systemic toxicity in rats.[61,62] However, high concentrations of AgNPs in the bloodstream may lead to severe toxicities[63] For example, intravenous administration of AgNPs at 20 mg/kg and above in Westar rats produced huge changes in WBC count, PLT count, hemoglobin, and RBC count, and the levels of liver function enzymes (including ALT, AST, ALP, GGT and

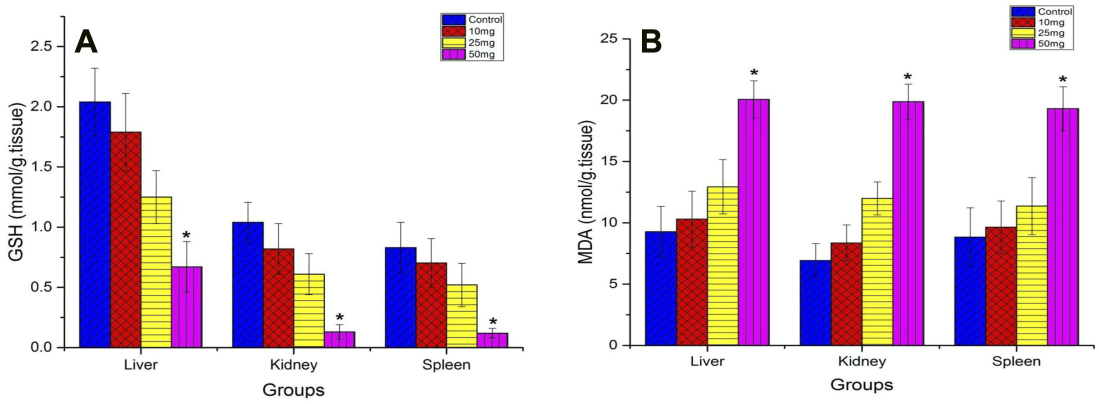

Figure 9 Tissue level of GSH (**A**) and MDA (**B**) in different groups. Data are represented as mean ± SEM. *Indicates significant difference from the corresponding control group at $P \leq 0.05$.
Abbreviations: GSH, glutathione; MDA, malondialdehyde.

TBil) were increased when 40 mg/kg of AgNPs were injected.[63] Hussain[64] detailed that AgNPs were highly toxic in rat liver cells. AgNPs reduced the mitochondrial activity leading to decrease the accessible vitality for cells.[65] In addition, some researchers confirmed that silver and silver salts are conveyed to the entire body, finally aggregating in the liver, kidney, and spleen; they also demonstrated that silver promotes the porosity of the cell layer to potassium and sodium, and disturbs the movement of Na-K-ATPase and mitochondria.[66,67] Tang and Xi[68] found that AgNPs cause liver and kidney toxicity, and a high dose prompts demise. Several previous studies revealed that AgNPs cause histopathological changes in the liver, spleen, and kidneys, demonstrating the tendency of silver ions to bind to thiol groups in the liver, prompting hepatocellular apoptosis. Experimental evidence has shown that metal oxide NPs induce DNA damage and apoptosis via ROS generation and oxidative damage.[45] Our study affirmed the renal and hepatocellular apoptosis incited by AgNPs by caspase-3 immunohistochemical responses which give a strong positive response in the group receiving the highest dose of Ch-AgNPs (50 mg/kg Ch-AgNPs). Decreased glutathione is important to evacuate peroxides,[69,70] so various types of NP could be dangerous in human and animal tissues.[71,72]

Lymphocyte and macrophage infiltration was uncovered as the key perceptions for AgNP-initiated morphological changes,[73,74] despite cell degeneration, regeneration, and necrosis. NPs introduced inflammation and immune response while interacting with tissues, which is a key component of nanotoxicity. In this way, the pathological alterations noticed in the spleen were associated with the immunotoxic effect of AgNPs. Our study showed a reduction in the serum levels of IgG in groups exposed to high doses of Ch-AgNPs without significant differences in levels of IgM. The reduction of IgG recommended immune suppression. Essentially, decrease of IgG recommends concealment of the functional immune system, prompting diminished protection from several diseases and infections. Together with a similar IgM, reduced IgG proposes that class switching from IgM to IgG is prevented by AgNP exposure. This impact is known to be initiated by immunosuppressive medications, for example, cyclosporine A and FK 506.[75] The histopathological observation of lymphoid cell atrophy and splenic or reticular cell hyperplasia in the group that received the highest dose, which is indicative for immune suppression, is in line with reduced IgG; this may suggest that impaired T-cell function is a cause for reduced IgG. It is outstanding that IgG is dependent on the assistance of T-helper just as B-cells.

In the present study, splenic and reticular cell hyperplasia observed in the group injected with 25 mg/kg Ch-AgNPs, as well as the lymphoid cell hyperplasia observed in the group injected with 10 mg/kg Ch-AgNPs, was confirmed by immunohistochemical examinations which found strong positive PCNA protein expression. Also, lymphoid cell apoptosis observed either in the periarterial lymphoid sheath or splenic lymphoid nodules in the splenic white pulp of rats injected with 50 mg/kg Ch-AgNPs was confirmed by immunohistochemical examinations, which found strong positive caspase-3 protein expression. Apoptosis (programmed cell death) is defined as a complex biological process which is important for regulating cell survival via removal of degenerated or injured cells[76] It is usually applicable to any type of cell death mediated

by an intracellular death program, regardless of the initiated mechanism[77] Caspase-3 is a well-known marker of apoptosis, and can be activated by both extrinsic and intrinsic apoptotic pathways and consequently lead to the breakdown of DNA.[78,79]

Even though the mechanisms by which Ch-AgNPs induce a proliferative response for splenocytes are not known, one possibility appears to be the generation of reactive oxygen species (oxidative stress) which may serve as mitogenic stimulators, initiating the cell cycle progression from G0 and through the G1-S restriction point.[80–83] In this study, there was a significant increase in the number of brown PCNA positive nuclei in splenic, reticular and lymphoid cells in both splenic red and white pulp in the group injected either with 25 or 10 mg/kg Ch-AgNPs. On the other hand, there was no significant difference in PCNA protein expression in the group injected with 50 mg/kg Ch-AgNPs compared with the control group. This may be due to extensive apoptosis observed in the spleen of rats in this group. PCNA is a marker of cell division and proliferation. PCNA was found in the cell nucleus and was directly involved in DNA synthesis84 Previous studies revealed that the AgNP-induced systemic and immunotoxic effect was initiated via the release of the products of oxidative stress such as different cytokines, ROS and at the same time the decrease of cellular antioxidants. These ROS of oxidative stress were detrimental and injurious to the cell compounds as lipid, protein, and membranes, eventually leading to inactivation of structural proteins, enzymes, and ion pumps, increased lipid peroxidation, impairment of cell functions, inflammation, cytolysis, interstitial fibrosis, mutation and damage to DNA, and apoptosis.[85,86]

In the present study, hematological parameters uncovered the immune suppression in the group administered with the highest dose of Ch-AgNPs. There was critical decline in total number of WBCs and lymphocytes, with minimum increase in blood monocytes in the group that received the highest dose. Our finding concurred with past investigations indicating the least modification in clinical biochemistry and hematology in rats receiving up to 50 mg/kg AgNPs.[87]

AgNPs were exceptionally industriousness in rodents and hard to be discharged from the body, and subsequently could applied its toxicity in a chronic state. Some previous studies uncovered that the Ag^+, not the NPs, was responsible for the major toxic effects of AgNPs regardless of the coating materials.[88,89] The majority of the harmful impacts brought about by AgNPs were contributed by the dissolved Ag^+,[90] and the conceivable mechanisms include actuation of lysosomal acid phosphatase activity, interruption of the actin cytoskeleton and incitement of phagocytosis, and hindrance of Na-K-ATPase. Later in vitro investigations further found that the toxicity of AgNPs chiefly relies on the intracellular discharge, not the silver ions liberated in the culture medium.[91,92] Lin et al[93] detailed that deadly bradyarrhythmias could be created with the presence of AgNPs, and further suggested that AgNPs contributed to their gross acute toxic effect on myocardial $\mathbf{I}_{Na}$ and $\mathbf{I}_{K1}$ channels, as the released Ag^+ was estimated to be less than 0.02%. Moreover, the organism-specific immune response incited by NPs should be given attention. It is further proposed that the inflammatory reaction might be vital for AgNP toxicity.[94]

Conclusion

This study aimed to provide a comprehensive insight into Ch-AgNP immunotoxicity in addition to studying the oxidative stress damage, and histopathological and immunohistochemical alterations induced in rats, to gain a better understanding of the potential risk of Ch-AgNP-containing medical materials. Hence, it was concluded that Ch-AgNPs induce dose-dependant adverse effects on rats.

Disclosure

The authors report no conflicts of interest in this work.

References

1. Nikalje AP. Nanotechnology and its applications in medicine. *Med Chem*. 2015;5:081–089. doi:10.4172/2161-0444
2. Marquis BJ, Love SA, Braun KL, Haynes CL. Analytical methods to assess nanoparticle toxicity. *Analyst*. 2009;134:425–439. doi:10.1039/b818082b
3. Love SA, Maurer-Jones MA, Thompson JW, Lin Y-S, Haynes CL. Assessing nanoparticle toxicity. *Annu Rev Anal Chem*. 2012;5:181–205. doi:10.1146/annurev-anchem-062011-143134
4. Fischer HC, Chan WC. Nanotoxicity: the growing need for in vivo study. *Curr Opin Biotechnol*. 2007;18:565–571. doi:10.1016/j.copbio.2007.11.008
5. de Lima R, Seabra AB, Durán N. Silver nanoparticles: a brief review of cytotoxicity and genotoxicity of chemically and biogenically synthesized nanoparticles. *J Appl Toxicol*. 2012;32(11):867–879. doi:10.1002/jat.v32.11
6. Beer C, Foldbjerg R, Hayashi Y, Sutherland DS, Autrup H. Toxicity of silver nanoparticles – nanoparticle or silver ion? *Toxicol Lett*. 2012;208(3):286–292. doi:10.1016/j.toxlet.2011.11.002
7. Rath G, Hussain T, Chauhan G, Garg T, Goyal AK. Collagen nanofiber containing silver nanoparticles for improved wound-healing applications. *J Drug Target*. 2016;24(6):520–529. doi:10.3109/1061186X.2015.1095922

8. Bergin IL, Wilding LA, Morishita M, et al. Effects of particle size and coating on toxicologic parameters, fecal elimination kinetics and tissue distribution of acutely ingested silver nanoparticles in a mouse model. *Nanotoxicology*. 2016;10(3):352–360. doi:10.3109/17435390.2015.1113322
9. Heydrnejad MS, Samani RJ, Aghaeivanda S. Toxic effects of silver nanoparticles on liver and some hematological parameters in male and female mice (Mus musculus). *Biol Trace Elem Res*. 2015;165(2):153–158. doi:10.1007/s12011-015-0247-1
10. Patlolla AK, Hackett D, Tchounwou PB. Silver nanoparticle-induced oxidative stress-dependent toxicity in Sprague-Dawley rats. *Mol Cell Biochem*. 2015;399(1–2):257–268. doi:10.1007/s11010-014-2252-7
11. Ji JH, Jung JH, Kim SS, et al. Twenty-eight-day inhalation toxicity study of silver nanoparticles in Sprague-Dawley rats. *Inhal Toxicol*. 2007;19(10):857–871. doi:10.1080/08958370701513113
12. Boudreau MD, Imam MS, Paredes AM, et al. Differential effects of silver nanoparticles and silver ions on tissue accumulation, distribution, and toxicity in the sprague dawley rat following daily oral gavage administration for 13 weeks. *Toxicol Sci*. 2016;150(1):131–160. doi:10.1093/toxsci/kfv318
13. Kim HR, Park YJ, Shin Da Y, Oh SM, Chung KH. Appropriate in vitro methods for genotoxicity testing of silver nanoparticles. *Environ Health Toxicol*. 2013;28:e2013003. doi:10.5620/eht.2013.28.e2013016
14. Su CK, Liu HT, Hsia SC, Sun YC. Quantitatively profiling the dissolution and redistribution of silver nanoparticles in living rats using a knotted reactor-based differentiation scheme. *Anal Chem*. 2014;86(16):8267–8274. doi:10.1021/ac501691z
15. Ishihara M, Nguyen VQ, Mori Y, Nakamura S, Hattori H. Adsorption of silver nanoparticles onto different surface structures of chitin/chitosan and correlations with antimicrobial activities. *Int J Mol Sci*. 2015;16(6):13973–13988. doi:10.3390/ijms160613973
16. Li CW, Wang Q, Li J, et al. Silver nanoparticles/chitosan oligosaccharide/poly(vinyl alcohol) nanofiber promotes wound healing by activating TGFbeta1/Smad signaling pathway. *Int J Nanomedicine*. 2016;11:373–386.
17. Wei D, Sun W, Qian W, Ye Y, Ma X. The synthesis of chitosan-based silver nanoparticles and their antibacterial activity. *Carbohydr Res*. 2009;344(17):2375–2382. doi:10.1016/j.carres.2009.09.001
18. Wang LS, Wang CY, Yang CH, et al. Synthesis and anti-fungal effect of silver nanoparticles-chitosan composite particles. *Int J Nanomedicine*. 2015;10:2685–2696.
19. Richardson SC, Kolbe HV, Duncan R. Potential of low molecular mass chitosan as a DNA delivery system: biocompatibility, body distribution and ability to complex and protect DNA. *Int J Pharm*. 1999;178(2):231–243. doi:10.1016/S0378-5173(98)00378-0
20. Li T, Albee B, Alemayehu M, et al. Comparative toxicity study of Ag, Au and Ag–au bimetallic nanoparticles on Daphnia magna. *Anal Bioanal Chem*. 2010;398(2):689–700. doi:10.1007/s00216-010-4234-2
21. Cao XL, Chena C, Ma YL, Zhao CS. Preparation of silver nanoparticles with antimicrobial activities and the researches of their biocompatibilities. *J Mater Sci Mater Med*. 2010;21:2861–2868. doi:10.1007/s10856-010-4133-2
22. Kim SY, Lee YM, Baik DJ, Kang JS. Toxic characteristics of methoxy poly (ethylene glycol)/poly (ε-caprolactone) nanospheres, in vitro and in vivo studies in the normal mice. *Biomaterials*. 2003;24:55–63. doi:10.1016/S0142-9612(02)00248-X
23. Leite-Silva VR, Le Lamer M, Sanchez WY, et al. The effect of formulation on the penetration of coated and uncoated zinc oxide nanoparticles into the viable epidermis of human skin in vivo. *Eur J Pharm Biopharm*. 2013;84:297–308. doi:10.1016/j.ejpb.2013.01.009
24. Goel R, Shah N, Visaria R, Paciotti GF, Bischof JC. Biodistribution of TNF-α-coated gold nanoparticles in an in vivo model system. *Nanomedicine*. 2009;4:401–410. doi:10.2217/nnm.09.21
25. Babu B, Nair RS, Angelo JM, Mathai V, Vineet RV. Evaluation of the efficacy of chitosan-silver nanocomposite on Candida albicans when compared to three different antifungal agents in combination with standard irrigation protocol: an ex vivo study. *Saudi Endod J*. 2017;7:87–91.
26. Liu Z, Huang GN. Exposure to silver nanoparticles does not affect cognitive outcome or hippocampal neurogenesis in adult mice. *Ecotoxicol Environ Saf*. 2013;87:124–130.
27. Bancroft JD, Gamble M. *Theories and Practice of Histological Techniques*. 6th ed. New York, London and Madrid: Churchil Livingstone; 2013.
28. Baliga R, Ueda N, Walker PD, Shah SV. Oxidant mechanisms in toxic acute renal failure. *Drug Metab Rev J*. 1999;31:971–997. doi:10.1081/DMR-100101947
29. Hsu SM, Raine L, Fanger H. The use of antiavidin antibody and avidin-biotin peroxidase complex in immunoperoxidase techniques. *Am J Clin Pathol*. 1981;75:816–821. doi:10.1093/ajcp/75.5.662
30. Ohkawa H, Ohishi W, Yagi K. Assay for lipid peroxides in animal tissues by thiobarbituric acid reaction. *Anal Bioche*. 1979;95(2):351–358. doi:10.1016/0003-2697(79)90738-3
31. Beutler E, Duron O, Kelly BM. Improved method for the determination of blood glutathione. *J Lab Clin Med*. 1963;61:882–890.
32. Klaine SJ, Alvarez PJJ, Batley GE. Nanomaterials in the environment: behaviour, fate, bioavailability and effects. *Environ Toxicol Chem*. 2008;27:1825–1851.
33. Ernest V, George Priya Doss C, Muthiah A, Mukherjee A, Chandrasekaran N. Genotoxicity assessment of low concentration Ag NPs to human peripheral blood lymphocytes. *Int J Pharm Pharm Sci*. 2013;5:377–381.
34. Kim TH, Kim M, Park HS, Shin US, Gong MS, Kim HW. Size-dependent cellular toxicity of silver nanoparticles. *J Biomed Mater Res A*. 2012;100:1033–1043. doi:10.1002/jbm.a.34053
35. Piao MJ1, Kang KA, Lee IK, et al. Silver nanoparticles induce oxidative cell damage in human liver cells through inhibition of reduced glutathione and induction of mitochondria-involved apoptosis. *Toxicol Lett*. 2011;201(1):92–100. doi:10.1016/j.toxlet.2010.12.010
36. Ranjbar A, Ataie Z, Khajavi F, Ghasemi H. Effects of silver nanoparticle (Ag NP) on oxidative stress biomarkers in rat. *Nanomed J*. 2013;1(3):205–211.
37. Ivask A, Kurvet I, Kasemets K, Blinova I, Aruoja V. Size-Dependent toxicity of silver nanoparticles to bacteria, yeast, algae, Crustaceans and mammalian cells in vitro. *PLoS One*. 2014;9:102–108. doi:10.1371/journal.pone.0102108
38. Ahamed M, Alsalhi MS, Siddiqui MK. Silver nanoparticle applications and human health. *Clin Chim Acta*. 2010;411(23–24):1841–1848. doi:10.1016/j.cca.2010.08.016
39. Dhawan A, Sharma V. Toxicity assessment of nanomaterials: methods and challenges. *Anal Bioanal Chem*. 2010;398(2):589–605. doi:10.1007/s00216-010-4234-2
40. Zhang T, Wang L, Chen Q, Chen C. Cytotoxic potential of silver nanoparticles. *Yonsei Med J*. 2014;55(2):283–291. doi:10.3349/ymj.2014.55.1.25
41. Christensen FM, Johnston HJ, Stone V, et al. Nano-silver feasibility and challenges for human health risk assessment based on open literature. *Nanotoxicology*. 2010;4:284e95.
42. Hashem MM, Salama MM, Mohammed FF, Tohamy AF, El Deeb KS. Metabolic profile and hepatoprotective effect of Aeschynomene elaphroxylon (Guill. & Perr.). *PLoS One*. 2019;14(1):e0210576. doi:10.1371/journal.pone.0210576
43. Nel A, Xia T, Mädler L, Li N. Toxic potential of materials at the nano level. *Science*. 2006;311(5761):622–627. doi:10.1126/science.1114397
44. Park EJ, Yi J, Kim Y, Choi K, Park K. Silver nanoparticles induce cytotoxicity by a Trojan-horse type mechanism. *Toxicol In Vitro*. 2010;24(3):872–878. doi:10.1016/j.tiv.2009.12.001
45. Asharani PV, Low Kah Mun G, Hande MP, Valiyaveettil S. Cytotoxicity and genotoxicity of silver nanoparticles in human cells. *ACS Nano*. 2009;3(2):279–290. doi:10.1021/nn800596w

46. Schlinkert P, Casals E, Boyles M, et al. The oxidative potential of differently charged silver and gold nanoparticles on three human lung epithelial cell types. *J Nanobiotechnology*. 2015;13:1. doi:10.1186/s12951-014-0062-4
47. Liu W, Wu Y, Wang C, et al. Impact of silver nanoparticles on human cells: effect of particle size. *Nanotoxicology*. 2010;4(3):319–330. doi:10.3109/17435390.2010.483745
48. Suliman YAO, Ali D, Alarifi S, Harrath AH, Mansour L, Alwasel SH. Evaluation of cytotoxic, oxidative stress, proinflammatory and genotoxic effect of silver nanoparticles in human lung epithelial cells. *Environ Toxicol*. 2015;30(2):149–160. doi:10.1002/tox.21880
49. El Mahdy MM, Eldin TA, Aly HS, Mohammed FF, Shaalan MI. Evaluation of hepatotoxic and genotoxic potential of silver nanoparticles in albino rats. *Exp Toxicol Pathol*. 2015;67(1):21–29. doi:10.1016/j.etp.2014.09.005
50. Hajji S, Khedir SB, Hamza-Mnif I, et al. Biomedical potential of chitosan-silver nanoparticles with special reference to antioxidant, antibacterial, hemolytic and in vivo cutaneous wound healing effects. *Biochim Biophys Acta Gen Subj*. 2019;1863(1):241–254. doi:10.1016/j.bbagen.2018.10.010
51. Fatima S, Arivarasu NA, Mahmood R. Vitamin C attenuates cisplatin-induced alterations in renal brush border membrane enzymes and phosphate transport. *Hum Exp Toxicol*. 2007;26:419–426. doi:10.1177/0960327106072389
52. Iseri S, Ercan F, Gedik N, Yuksel M, Alican I. Simvastatin attenuates cisplatin-induced kidney and liver damage in rats. *Toxicology*. 2007;230:256–264. doi:10.1016/j.tox.2006.11.073
53. Anwar MF, Yadav D, Rastogi S, et al. Modulation of liver and kidney toxicity by herb Withania somnifera for silver nanoparticles: a novel approach for harmonizing between safety and use of nanoparticles. *Protoplasma*. 2015;252(2):547–558. doi:10.1007/s00709-014-0701-5
54. Zhai HJ, Sun DW, Wang HS. Catalytic properties of silica/silver nanocomposites. *J Nanosci Nanotechnol*. 2006;6(7):1968–1972.
55. Xu L, Shao A, Zhao Y, et al. Neurotoxicity of silver nanoparticles in rat brain after intragastric exposure. *J Nanosci Nanotechnol*. 2015;15(6):4215–4223. doi:10.1166/jnn.2015.9612
56. Parang Z, Moghadamnia D. Effects of silver nanoparticles on the functional tests of liver and its histological changes in adult male rats. *Nanomed Res J*. 2018;3(3):146–153.
57. Jiménez-Lamana J, Laborda F, Bolea E, et al. An insight into silver nanoparticles bioavailability in rats. *Metallomics*. 2014;6(12):2242–2249. doi:10.1039/C4MT00200H
58. Loeschner K, Hadrup N, Qvortrup K, et al. Distribution of silver in rats following 28 days of repeated oral exposure to silver nanoparticles or silver acetate. *Part Fibre Toxicol*. 2011;8:18. doi:10.1186/1743-8977-8-18
59. Al Gurabi MA, Ali D, Alkahtani S, Alarifi S. In vivo DNA damaging and apoptotic potential of silver nanoparticles in Swiss albino mice. *Onco Targets Ther*. 2015;29(8):295–302.
60. Guo H, Zhang J, Boudreau M, et al. Intravenous administration of silver nanoparticles causes organ toxicity through intracellular ROS-related loss of inter-endothelial junction. *Part Fibre Toxicol*. 2016;29:13–21.
61. Hong JS, Kim S, Lee SH, et al. Combined repeated-dose toxicity study of silver nanoparticles with the reproduction/developmental toxicity screening test. *Nanotoxicology*. 2014;8(4):349–362. doi:10.3109/17435390.2013.780108
62. Smock KJ, Schmidt RL, Hadlock G, Stoddard G, Grainger DW, Munger MA. Assessment of orally dosed commercial silver nanoparticles on human ex vivo platelet aggregation. *Nanotoxicology*. 2014;8(3):328–333. doi:10.3109/17435390.2013.788749
63. Tiwari DK, Jin T, Behari J. Dose-dependent in-vivo toxicity assessment of silver nanoparticle in Wistar rats. *Toxicol Mech Methods*. 2011;21(1):13–24. doi:10.3109/15376516.2011.568980
64. Hussain SM. In vitro toxicity of nanoparticles in BRL 3A rat liver cells. *Toxicol In Vitro*. 2005;19:975–983. doi:10.1016/j.tiv.2005.06.034
65. Chen X, Schluesener HJ. Nanosilver: a nanoproduct in medical application. *Toxicol Lett*. 2008;176(1):1–12. doi:10.1016/j.toxlet.2007.10.004
66. Oberdo Rster G. Increased pulmonary toxicity of ultrafine particles Lung lavage studies. *J Aerosol Sci*. 1990;21:384–387. doi:10.1016/0021-8502(90)90065-6
67. Lam CW. A review of carbon nanotube toxicity and assessment of potential occupational and environmental health risk. *Crit Rev Toxicol*. 2006;36:189–217.
68. Tang J, Xi T. Status of biological evaluation on silver nanoparticles. *Sheng wu yi xue gong cheng xue za zhi*. 2008;25:958–961.
69. Hendi A. Silver nanoparticles mediate diffrential responses in some of liver and kidney functions during skin woud healing. *J King Saud Univ Sci*. 2010;23(1):47–52. doi:10.1016/j.jksus.2010.06.006
70. Campen MJ, McDonald JD, Gigliotti AP, Seilkop SK, Reed MD, Benson JM. Cardiovascular effects of inhaled diesel exhaust in spontaneously hypertensive-rate. *Cardiovas Toxicol*. 2003;3:353–361. doi:10.1385/CT:3:4:353
71. Miura N, Shinohara Y. Cytotoxic effect and apoptosis induction by silver nanoparticles in hela cells. *Biochem Biophys Res Commun*. 2009;390(3):733–737. doi:10.1016/j.bbrc.2009.11.007
72. Choi JE, Kim S, Ahn JH, et al. Induction of oxidative stress and apoptosis by silver nanoparticles in the liver of adult zebrafish. *Aquat Toxicol*. 2010;100(2):151–159. doi:10.1016/j.aquatox.2009.12.012
73. Yun JW, Kim SH, You JR, et al. Comparative toxicity of silicon dioxide, silver and iron oxide nanoparticles after repeated oral administration to rats. *J Appl Toxicol*. 2015;35(6):681–693. doi:10.1002/jat.3034
74. Chuang HC, Hsiao TC, Wu CK, et al. Allergenicity and toxicology of inhaled silver nanoparticles in allergen-provocation mice models. *Int J Nanomedicine*. 2013;8:4495–4506. doi:10.2147/IJN.S37465
75. Thomson AW, Propper DJ, Woo J, Whiting PH, Milton JI, Macleod AM. Comparative effects of rapamycin, FK 506 and cyclosporine on antibody production, lymphocyte populations and immunoglobulin isotype switching in the rat. *Immunopharmacol Immunotoxicol*. 1993;15:355–369. doi:10.3109/08923979309035233
76. Kuranaga E. Beyond apoptosis: caspase regulatory mechanisms and functions in vivo. *Genes Cells*. 2012;17:83–97. doi:10.1111/j.1365-2443.2011.01579.x
77. Pawlina W. *Histology a Text and Atlas with Correlated Cell and Molecular Biology*. 7th ed. Philadelphia, Baltimore, New York, London: Wolters Kluwer; 2016:698–699, pp 91–94 and P. 720.
78. Dai C, Tang S, Deng S, et al. Lycopene attenuates colistin-induced nephrotoxicity in mice via activation of the Nrf2/HO-1 pathway. *Antimicrob Agents Chemother*. 2015;59:579–585. doi:10.1128/AAC.03925-14
79. Kumar V, Abbas AK, Aster JC, Editors. *Robbin's Basic Pathology*. 9th ed. Philadelphia: Elsevier Saunders Company; 2013:18–22.
80. Emmendoerffer A, Hecht M, Boeker T, Mueller M, Heinrich U. Role of inflammation in chemical-induced lung cancer. *Toxicol Lett*. 2000;112–113:185–191. doi:10.1016/S0378-4274(99)00285-4
81. Brown KE, Mathahs MM, Broadhurst KA, Weydert J. Chronic iron overload stimulates hepatocyte proliferation and cyclin D1 expression in rodent liver. *Transl Res*. 2006;148:55–62. doi:10.1016/j.trsl.2006.03.002
82. Menon SG, Goswami PC. A redox cycle within the cell cycle: ring in the old with the new. *Oncogene*. 2007;26:1101–1109. doi:10.1038/sj.onc.1209895
83. Sarsour EH, Kumar MG, Chaudhuri L, Kalen AL, Goswami PC. Redox control of the cell cycle in health and disease. *Antioxid Redox Signal*. 2009;11:2985–3011. doi:10.1089/ars.2009.2513
84. Hegazy R, Salama A, Mansour D, Hassan A. Renoprotective effect of lactoferrin against chromium-induced acute kidney injury in rats: involvement of IL-18 and IGF-1 inhibition. *PLoS One*. 2016;11(3):e0151486. 1–18. doi:10.1371/journal.pone.0151486
85. Oberdörster G, Kane AB, Klaper RD, Hurt RH. Nanotoxicology. In: Klaassen CD, editor. *Casarett and Doull's Toxicology, the Basic Science of Poisons*. 8th ed. New York, Chicago, San Francisco, Lisbon, London: Ch 28, McGraw-Hill Education; 2013:1189–1229.

86. Grande F, Tucci P. Titanium dioxide nanoparticles: a risk for human health? *Mini Rev Med Chem*. 2016;16(9):762–769.
87. Vandebriel RJ, Tonk ECM, de la Fonteyne-Blankestijn LJ, et al. Immunotoxicity of silver nanoparticles in an intravenous 28-day repeated-dose toxicity study in rats. *Part Fibre Toxicol*. 2014;11:21. doi:10.1186/1743-8977-11-21
88. Sakamoto M, Ha JY, Yoneshima S, Kataoka C, Tatsuta H, Kashiwada S. Free silver ion as the main cause of acute and chronic toxicity of silver nanoparticles to cladocerans. *Arch Environ Contam Toxicol*. 2015;68(3):500–509. doi:10.1007/s00244-014-0091-x
89. Hadrup N, Loeschner K, Bergstrom A, et al. Subacute oral toxicity investigation of nanoparticulate and ionic silver in rats. *Arch Toxicol*. 2012;86(4):543–551. doi:10.1007/s00204-011-0763-5
90. Katsumiti A, Gilliland D, Arostegui I, Cajaraville MP. Mechanisms of toxicity of Ag nanoparticles in comparison to bulk and ionic Ag on mussel hemocytes and gill cells. *PLoS One*. 2015;10(6):e0129039. doi:10.1371/journal.pone.0129039
91. De Matteis V, Malvindi MA, Galeone A, et al. Negligible particle-specific toxicity mechanism of silver nanoparticles: the role of Ag^{+} ion release in the cytosol. *Nanomedicine*. 2015;11(3):731–739. doi:10.1016/j.nano.2014.11.002
92. Sabella S, Carney RP, Brunetti V, et al. A general mechanism for intracellular toxicity of metal-containing nanoparticles. *Nanoscale*. 2014;6(12):7052–7061. doi:10.1039/c4nr01234h
93. Lin CX, Yang SY, Gu JL, Meng J, Xu HY, Cao JM. The acute toxic effects of silver nanoparticles on myocardial transmembrane potential, INa and IK1 channels and heart rhythm in mice. *Nanotoxicology*. 2017;1–11. doi:10.1080/17435390.2017.1367047
94. Xu L, Shi C, Shao A, et al. Toxic responses in rat embryonic cells to silver nanoparticles and released silver ions as analyzed via gene expression profiles and transmission electron microscopy. *Nanotoxicology*. 2015;9(4):513–522. doi:10.3109/17435390.2014.894150